

Variability of the ^{15}N Chemical Shielding Tensors in the B3 Domain of Protein G from ^{15}N Relaxation Measurements at Several Fields. Implications for Backbone Order Parameters.

By Jennifer B. Hall and David Fushman

Supporting Table 1. A list of various ^{15}N relaxation and cross-correlation experiments used in this study and the relevant relaxation delays. Shown in the last column are the durations of relaxation-active delays in the relaxation and cross-correlation measurements or the relaxation delay between successive scans in hetero-NOE experiments.

Frequency	Measured rate	Relaxation delay
400 MHz (9.4 Tesla)	R_1	432, 432, 4, 432, 432, 4 ms
	R_2	280, 280, 8, 280, 280, 8 ms
	NOE	4.5 s
	η_{xy}	0, 21.27, 31.91, 42.53, 53.19 ms
	η_z	0, 100, 200, 250, 300, 350 ms
500 MHz (11.7 Tesla)	R_1	504, 504, 4, 504, 504, 4 ms
	R_2	248, 248, 8, 248, 248, 8 ms
	NOE	4.69 s
	η_{xy}	0, 31.91, 26.59, 42.55, 53.19 ms
	η_z	0, 100, 200, 250, 300, 350 ms
600 MHz (14.1 Tesla)	R_1	440, 440, 4, 440, 440 ms
	R_2	264, 264, 8, 264, 264 ms
	NOE	5 s
	η_{xy}	26.59, 31.91, 37.23, 42.55, 53.19 ms
	η_z	0, 100, 150, 200, 300, 400 ms
700 MHz (16.4 Tesla)	R_1	620, 620, 4, 620, 620, 4 ms

	R ₂	264, 264, 8, 264, 264, 8 ms
	NOE	4 s
	η_{xy}	26.59, 31.91, 37.23, 42.55, 53.19 ms
800 MHz (18.8 Tesla)	R ₁	672, 672, 4, 672, 672, 4 ms
	R ₂	248, 248, 8, 248, 248, 8 ms
	NOE	4.7 s
	η_{xy}	26.59, 31.91, 37.23, 42.55, 53.19 ms

Supporting Table 2. ¹⁵N Relaxation and Cross-Correlation Data in GB3. All rates are in units of s⁻¹.

Res #	R ₁ (9.4T)	δR_1 (9.4T)	R ₁ (11.7T)	δR_1 (11.7T)	R ₁ (14.1T)	δR_1 (14.1T)	R ₁ (16.4T)	δR_1 (16.4T)	R ₁ (18.8T)	δR_1 (18.8T)
2	3.05	0.05	2.67	0.04	2.30	0.04	2.18	0.03	1.91	0.03
3	2.98	0.04	2.67	0.03	2.28	0.02	2.05	0.03	1.85	0.03
4	3.04	0.03	2.74	0.02	2.36	0.02	2.10	0.02	1.90	0.05
5	3.08	0.06	2.69	0.02	2.39	0.02	2.15	0.01	1.89	0.03
6	3.08	0.03	2.61	0.02	2.36	0.02	2.01	0.01	1.86	0.03
7	3.02	0.05	2.63	0.01	2.31	0.04	1.96	0.01	1.76	0.03
8	3.00	0.04	2.58	0.01	2.33	0.02	1.96	0.04	1.75	0.03
9	2.95	0.02	2.53	0.01	2.29	0.02	2.09	0.01	1.90	0.01
10	2.82	0.03	2.54	0.01	2.22	0.01	2.04	0.01	1.92	0.01
11	2.73	0.05	2.40	0.01	2.10	0.02	1.96	0.02	1.88	0.00
12	2.29	0.02	2.07	0.01	1.87	0.01	1.73	0.02	1.67	0.00
13	2.80	0.03	2.39	0.01	2.13	0.02	1.86	0.01	1.66	0.02
14.	2.56	0.03	2.22	0.02	2.06	0.06	1.83	0.02	1.74	0.02
16	2.93	0.04	2.54	0.03	2.26	0.04	2.03	0.04	1.81	0.01
17	2.92	0.05	2.57	0.02	2.21	0.03	2.09	0.04	1.94	0.06

18	3.00	0.02	2.61	0.03	2.32	0.06	2.06	0.04	1.91	0.02
19	2.77	0.05	2.44	0.05	2.13	0.02	1.97	0.03	1.80	0.02
20.	2.80	0.02	2.41	0.01	2.22	0.04	1.83	0.01	1.61	0.02
21	3.03	0.02	2.66	0.01	2.28	0.02	2.11	0.02	1.95	0.01
22	3.00	0.03	2.64	0.02	2.34	0.06	2.16	0.04	2.01	0.01
23	3.11	0.04	2.65	0.03	2.35	0.03	2.05	0.02	1.80	0.05
24	2.93	0.03	2.51	0.02	2.19	0.05	1.94	0.02	1.79	0.02
26	3.03	0.05	2.50	0.01	2.39	0.06	1.79	0.03	1.58	0.02
28	3.08	0.04	2.65	0.04	2.26	0.11	2.03	0.04	1.82	0.02
29	3.18	0.02	2.59	0.03	2.32	0.06	2.01	0.04	1.76	0.02
30	3.20	0.02	2.78	0.04	2.43	0.07	2.21	0.02	2.04	0.04
31	3.24	0.04	2.77	0.04	2.31	0.06	2.13	0.01	1.93	0.05
32	3.13	0.05	2.71	0.04	2.35	0.03	2.07	0.04	1.96	0.05
33	3.19	0.05	2.77	0.01	2.44	0.06	2.16	0.02	1.90	0.04
34	3.18	0.02	2.74	0.05	2.42	0.02	2.09	0.02	1.91	0.03
36	3.13	0.04	2.58	0.02	2.27	0.05	1.99	0.01	1.81	0.01
37	2.95	0.03	2.56	0.03	2.22	0.02	2.03	0.05	1.83	0.03
38	2.98	0.03	2.59	0.01	2.28	0.01	2.10	0.01	1.86	0.01
39	2.91	0.02	2.52	0.01	2.28	0.02	2.02	0.01	1.85	0.02
40	2.60	0.02	2.27	0.00	2.00	0.01	1.83	0.03	1.66	0.01
41	2.18	0.01	1.96	0.01	1.72	0.02	1.59	0.02	1.44	0.01
42	2.90	0.02	2.57	0.03	2.28	0.02	1.96	0.02	1.79	0.02
43	3.10	0.03	2.76	0.02	2.36	0.02	2.33	0.04	2.13	0.02
44	3.00	0.02	2.67	0.01	2.38	0.02	2.12	0.02	1.88	0.02
45	2.87	0.04	2.51	0.05	2.25	0.02	2.05	0.01	1.92	0.02
46	3.00	0.05	2.61	0.02	2.37	0.04	2.09	0.02	1.93	0.04
47	2.89	0.02	2.54	0.01	2.21	0.01	2.04	0.01	1.90	0.01
48	2.79	0.04	2.43	0.03	2.12	0.01	1.96	0.01	1.84	0.01

49	2.89	0.03	2.48	0.01	2.21	0.02	2.00	0.03	1.91	0.03
50	3.06	0.03	2.71	0.01	2.38	0.02	2.25	0.01	2.16	0.02
51	2.96	0.05	2.61	0.03	2.32	0.03	2.03	0.02	1.84	0.03
52	3.17	0.05	2.98	0.02	2.37	0.04	2.59	0.06	2.47	0.10
53	3.06	0.06	2.67	0.04	2.33	0.03	2.20	0.01	2.02	0.05
54	3.16	0.03	2.66	0.02	2.42	0.02	2.17	0.01	2.04	0.03
55	3.01	0.03	2.62	0.05	2.32	0.06	2.05	0.01	1.85	0.02
56	3.00	0.04	2.62	0.01	2.34	0.02	2.15	0.01	2.00	0.03

Res #	R ₂	δR ₂								
	(9.4T)	(9.4T)	(11.7T)	(11.7T)	(14.1T)	(14.1T)	(16.4T)	(16.4T)	(18.8T)	(18.8T)
2	4.93	0.08	4.91	0.04	5.06	0.04	5.39	0.03	5.71	0.01
3	4.71	0.10	4.73	0.05	4.78	0.04	5.05	0.05	5.42	0.06
4	4.98	0.07	4.99	0.08	5.10	0.03	5.27	0.03	5.60	0.10
5	4.87	0.07	4.92	0.10	5.20	0.11	5.25	0.08	5.54	0.07
6	4.83	0.06	4.81	0.03	5.02	0.05	5.14	0.06	5.38	0.10
7	4.67	0.07	4.72	0.07	4.85	0.06	4.91	0.13	5.19	0.09
8	4.67	0.07	4.65	0.04	5.02	0.05	5.05	0.02	5.29	0.11
9	4.76	0.06	4.66	0.02	4.90	0.04	5.11	0.01	5.54	0.01
10	4.50	0.03	4.40	0.01	4.78	0.03	5.11	0.02	5.44	0.01
11	4.43	0.05	4.54	0.01	4.65	0.03	4.98	0.02	5.43	0.01
12	3.52	0.04	3.80	0.01	3.78	0.02	3.92	0.01	3.98	0.01
13	4.29	0.04	4.34	0.04	4.66	0.04	4.52	0.03	4.84	0.04
14	4.03	0.04	4.10	0.07	4.27	0.10	4.51	0.10	4.92	0.11
16	4.65	0.09	4.54	0.09	4.78	0.16	4.88	0.09	5.34	0.13
17	4.54	0.05	4.53	0.08	4.75	0.02	5.19	0.11	5.48	0.08
18	4.70	0.04	4.70	0.04	4.97	0.09	5.10	0.09	5.51	0.02

19	4.42	0.05	4.47	0.08	4.53	0.02	4.78	0.05	5.15	0.08
20	4.40	0.03	4.46	0.02	4.58	0.05	4.55	0.02	4.65	0.01
21	4.82	0.06	4.85	0.01	4.94	0.02	5.30	0.01	5.76	0.01
22	5.04	0.04	4.87	0.11	5.40	0.17	5.79	0.13	5.98	0.16
23	5.13	0.06	5.16	0.08	5.34	0.05	5.43	0.08	5.91	0.13
24	4.96	0.06	5.09	0.10	5.24	0.05	5.70	0.02	6.08	0.16
26	4.99	0.06	4.87	0.16	5.32	0.17	5.03	0.10	5.12	0.21
28	5.40	0.08	5.46	0.07	5.48	0.17	5.92	0.07	6.25	0.20
29	5.27	0.07	5.31	0.10	5.54	0.23	5.66	0.04	5.92	0.21
30	5.37	0.05	5.44	0.06	5.67	0.10	6.14	0.02	6.61	0.14
31	5.51	0.04	5.59	0.04	5.90	0.09	6.20	0.06	6.72	0.15
32	5.51	0.11	5.56	0.06	5.76	0.19	6.08	0.13	6.64	0.09
33	5.26	0.05	5.27	0.14	5.62	0.15	5.93	0.15	6.57	0.17
34	5.31	0.07	5.42	0.10	5.70	0.03	5.97	0.02	6.51	0.20
36	5.26	0.08	5.32	0.04	5.62	0.14	5.72	0.02	6.03	0.02
37	4.93	0.05	4.72	0.07	5.05	0.07	5.35	0.11	5.59	0.03
38	4.89	0.04	4.97	0.02	5.17	0.03	5.57	0.02	5.50	0.01
39	5.24	0.04	5.30	0.01	5.76	0.02	6.12	0.02	6.63	0.01
40	4.46	0.04	4.37	0.01	4.69	0.02	5.31	0.01	4.98	0.01
41	3.41	0.02	3.39	0.01	3.55	0.01	3.91	0.01	3.73	0.00
42	4.78	0.09	4.84	0.18	4.98	0.11	5.27	0.09	5.59	0.11
43	4.82	0.06	5.03	0.08	5.21	0.09	5.64	0.06	6.15	0.03
44	4.72	0.05	4.83	0.10	5.05	0.03	5.13	0.06	5.57	0.03
45	4.52	0.07	4.62	0.08	4.75	0.02	5.03	0.04	5.37	0.04
46	4.61	0.06	4.69	0.06	4.85	0.08	5.14	0.09	5.64	0.11
47	4.61	0.04	4.74	0.01	4.70	0.02	4.88	0.02	5.16	0.01
48	4.58	0.03	4.47	0.01	4.75	0.02	5.23	0.01	5.64	0.01
49	4.69	0.08	4.80	0.01	4.86	0.02	4.98	0.02	4.21	0.07

50	4.62	0.04	4.59	0.01	5.07	0.02	5.44	0.02	5.80	0.01
51	4.66	0.04	4.65	0.06	4.91	0.06	5.02	0.05	5.40	0.02
52	4.99	0.07	5.39	0.10	5.22	0.19	6.35	0.06	7.10	0.25
53	4.73	0.09	4.97	0.07	4.99	0.06	5.41	0.08	5.88	0.11
54	4.86	0.08	4.86	0.08	5.17	0.04	5.32	0.04	5.74	0.02
55	4.79	0.06	4.85	0.06	5.00	0.03	5.30	0.03	5.49	0.02
56	4.97	0.04	4.95	0.01	5.17	0.02	5.37	0.02	4.70	0.06

Res #	NOE	δ NOE	NOE	δ NOE	NOE	δ NOE	NOE	δ NOE	NOE	δ NOE
	(9.4T)	(9.4T)	(11.7T)	(11.7T)	(14.1T)	(14.1T)	(16.4T)	(16.4T)	(18.8T)	(18.8T)
2	0.50	0.01	0.59	0.01	0.64	0.01	0.67	0.01	0.72	0.01
3	0.52	0.01	0.62	0.01	0.70	0.01	0.73	0.01	0.76	0.01
4	0.53	0.01	0.64	0.01	0.69	0.01	0.75	0.01	0.77	0.01
5	0.52	0.01	0.62	0.01	0.70	0.01	0.74	0.01	0.76	0.01
6	0.53	0.01	0.63	0.01	0.70	0.01	0.74	0.01	0.75	0.01
7	0.51	0.01	0.62	0.01	0.71	0.01	0.72	0.01	0.77	0.01
8	0.50	0.01	0.61	0.01	0.70	0.01	0.74	0.01	0.80	0.01
9	0.47	0.01	0.63	0.01	0.67	0.01	0.74	0.01	0.76	0.01
10	0.43	0.00	0.56	0.01	0.64	0.01	0.70	0.01	0.72	0.01
11	0.39	0.01	0.53	0.01	0.61	0.01	0.65	0.01	0.71	0.01
12	0.37	0.01	0.50	0.01	0.59	0.01	0.66	0.01	0.73	0.01
13	0.43	0.01	0.55	0.01	0.63	0.01	0.69	0.01	0.74	0.01
14	0.47	0.00	0.58	0.01	0.65	0.01	0.67	0.01	0.70	0.01
16	0.51	0.01	0.63	0.01	0.69	0.01	0.72	0.01	0.76	0.01
17	0.53	0.01	0.64	0.01	0.69	0.01	0.74	0.01	0.78	0.01
18	0.52	0.01	0.62	0.01	0.70	0.01	0.73	0.01	0.75	0.01
19	0.52	0.01	0.64	0.01	0.70	0.01	0.75	0.01	0.78	0.01

20	0.48	0.01	0.61	0.01	0.69	0.01	0.74	0.01	0.77	0.01
21	0.51	0.01	0.61	0.01	0.68	0.01	0.73	0.01	0.85	0.01
22	0.53	0.01	0.71	0.01	0.69	0.01	0.77	0.01	0.88	0.01
23	0.58	0.01	0.68	0.01	0.75	0.01	0.80	0.01	0.82	0.01
24	0.59	0.00	0.68	0.01	0.74	0.01	0.77	0.01	0.79	0.01
26	0.57	0.01	0.65	0.01	0.74	0.01	0.75	0.01	0.79	0.01
28	0.60	0.01	0.69	0.01	0.75	0.01	0.79	0.01	0.80	0.01
29	0.59	0.01	0.69	0.01	0.74	0.01	0.79	0.01	0.81	0.01
30	0.61	0.00	0.69	0.01	0.74	0.01	0.79	0.01	0.82	0.01
31	0.61	0.01	0.71	0.01	0.76	0.01	0.78	0.01	0.83	0.01
32	0.60	0.01	0.69	0.01	0.75	0.01	0.78	0.01	0.82	0.01
33	0.60	0.01	0.70	0.01	0.74	0.01	0.78	0.01	0.82	0.01
34	0.59	0.00	0.69	0.01	0.74	0.01	0.79	0.01	0.81	0.01
36	0.57	0.00	0.66	0.01	0.77	0.01	0.80	0.01	0.81	0.01
37	0.53	0.01	0.67	0.01	0.73	0.01	0.77	0.01	0.81	0.01
38	0.55	0.01	0.64	0.01	0.72	0.01	0.76	0.01	0.86	0.01
39	0.54	0.01	0.63	0.01	0.71	0.01	0.76	0.01	0.83	0.01
40	0.40	0.00	0.52	0.01	0.59	0.01	0.65	0.01	0.73	0.01
41	0.19	0.00	0.33	0.01	0.43	0.00	0.51	0.01	0.59	0.01
42	0.56	0.01	0.64	0.01	0.72	0.01	0.74	0.01	0.76	0.01
43	0.54	0.01	0.65	0.01	0.71	0.01	0.76	0.01	0.79	0.01
44	0.52	0.01	0.63	0.01	0.71	0.01	0.75	0.01	0.77	0.01
45	0.55	0.00	0.67	0.01	0.73	0.01	0.78	0.01	0.81	0.01
46	0.54	0.01	0.64	0.01	0.72	0.01	0.76	0.01	0.78	0.01
47	0.50	0.00	0.65	0.01	0.71	0.01	0.75	0.01	0.88	0.01
48	0.51	0.00	0.72	0.01	0.70	0.01	0.75	0.01	0.78	0.01
49	0.52	0.01	0.66	0.01	0.76	0.01	0.77	0.01	0.82	0.01
50	0.52	0.01	0.67	0.01	0.71	0.01	0.79	0.01	0.79	0.01

51	0.53	0.01	0.64	0.01	0.72	0.01	0.75	0.01	0.78	0.01
52	0.57	0.01	0.68	0.01	0.74	0.01	0.80	0.01	0.81	0.01
53	0.54	0.01	0.65	0.01	0.72	0.01	0.75	0.01	0.77	0.01
54	0.52	0.01	0.62	0.01	0.70	0.01	0.72	0.01	0.76	0.01
55	0.53	0.01	0.63	0.01	0.72	0.01	0.74	0.01	0.78	0.01
56	0.49	0.01	0.61	0.01	0.68	0.01	0.74	0.01	0.76	0.01

Res #	η_z (9.4T)	$\delta\eta_z$ (9.4T)	η_z (11.7T)	$\delta\eta_z$ (11.7T)	η_z (14.1T)	$\delta\eta_z$ (14.1T)	η_z (16.4T)	$\delta\eta_z$ (16.4T)	η_z (18.8T)	$\delta\eta_z$ (18.8T)
2	1.56	0.03	1.50	0.02	1.48	0.02	-	-	-	-
3	1.62	0.02	1.66	0.01	1.66	0.02	-	-	-	-
4	1.84	0.02	1.91	0.02	1.90	0.03	-	-	-	-
5	1.65	0.01	1.65	0.02	1.63	0.03	-	-	-	-
6	1.86	0.02	1.87	0.02	1.83	0.03	-	-	-	-
7	1.44	0.02	1.50	0.02	1.43	0.02	-	-	-	-
8	1.52	0.03	1.51	0.02	1.46	0.03	-	-	-	-
9	1.29	0.01	1.32	0.03	1.24	0.03	-	-	-	-
10	1.46	0.01	1.50	0.02	1.58	0.02	-	-	-	-
11	1.27	0.02	1.52	0.01	1.22	0.01	-	-	-	-
12	1.29	0.01	1.43	0.03	1.09	0.02	-	-	-	-
13	1.46	0.03	1.52	0.02	1.46	0.02	-	-	-	-
14	1.32	0.01	1.36	0.01	1.34	0.03	-	-	-	-
16	1.56	0.02	1.58	0.01	1.60	0.03	-	-	-	-
17	1.61	0.03	1.67	0.03	1.62	0.04	-	-	-	-
18	1.67	0.02	1.64	0.01	1.69	0.03	-	-	-	-
19	1.70	0.02	1.78	0.01	1.73	0.02	-	-	-	-
20	1.47	0.01	1.53	0.02	1.37	0.01	-	-	-	-

21	1.38	0.01	1.55	0.01	1.33	0.01	-	-	-	-
22	1.61	0.02	1.62	0.01	1.59	0.03	-	-	-	-
23	1.45	0.01	1.45	0.02	1.41	0.01	-	-	-	-
24	1.66	0.01	1.64	0.01	1.54	0.03	-	-	-	-
26	1.39	0.02	1.43	0.01	1.36	0.01	-	-	-	-
28	1.66	0.03	1.58	0.02	1.51	0.03	-	-	-	-
29	1.78	0.01	1.78	0.02	1.74	0.03	-	-	-	-
30	1.81	0.04	1.82	0.03	1.75	0.01	-	-	-	-
31	1.76	0.02	1.74	0.01	1.69	0.03	-	-	-	-
32	1.79	0.03	1.81	0.03	1.71	0.01	-	-	-	-
33	1.82	0.03	1.82	0.01	1.79	0.03	-	-	-	-
34	1.81	0.02	1.83	0.03	1.76	0.03	-	-	-	-
36	1.69	0.01	1.63	0.04	1.52	0.04	-	-	-	-
37	1.68	0.02	1.69	0.02	1.62	0.03	-	-	-	-
38	1.58	0.03	1.64	0.01	1.42	0.02	-	-	-	-
39	1.56	0.02	1.65	0.01	1.71	0.04	-	-	-	-
40	1.36	0.02	1.35	0.03	1.25	0.01	-	-	-	-
41	0.89	0.01	0.88	0.02	0.56	0.01	-	-	-	-
42	1.61	0.02	1.59	0.03	1.59	0.03	-	-	-	-
43	1.77	0.03	1.81	0.01	1.77	0.04	-	-	-	-
44	1.68	0.02	1.68	0.02	1.66	0.01	-	-	-	-
45	1.65	0.00	1.68	0.02	1.68	0.03	-	-	-	-
46	1.70	0.03	1.77	0.02	1.68	0.02	-	-	-	-
47	1.48	0.02	1.63	0.01	1.34	0.03	-	-	-	-
48	1.41	0.02	1.55	0.01	1.60	0.03	-	-	-	-
49	1.32	0.01	1.36	0.00	1.31	0.02	-	-	-	-
50	1.80	0.04	1.93	0.02	1.85	0.01	-	-	-	-
51	1.56	0.03	1.63	0.01	1.57	0.03	-	-	-	-

52	1.99	0.02	2.08	0.01	2.01	0.04	-	-	-	-
53	1.93	0.03	1.91	0.03	1.94	0.02	-	-	-	-
54	2.02	0.03	2.08	0.02	1.99	0.02	-	-	-	-
55	1.71	0.02	1.80	0.02	1.77	0.03	-	-	-	-
56	1.67	0.02	1.71	0.04	1.54	0.01	-	-	-	-

Res #	η_{xy}	$\delta\eta_{xy}$								
	(9.4T)	(9.4T)	(11.7T)	(11.7T)	(14.1T)	(14.1T)	(16.4T)	(16.4T)	(18.8T)	(18.8T)
2	2.58	0.04	3.09	0.08	3.43	0.09	-	-	3.84	0.04
3	2.64	0.05	3.19	0.06	3.52	0.09	-	-	4.50	0.04
4	3.04	0.07	3.60	0.05	4.06	0.07	-	-	5.05	0.04
5	2.61	0.07	3.13	0.04	3.54	0.03	-	-	4.35	0.07
6	3.05	0.02	3.63	0.05	3.99	0.09	-	-	5.05	0.04
7	2.35	0.02	2.75	0.02	3.08	0.06	-	-	3.89	0.04
8	2.42	0.03	2.94	0.07	3.33	0.04	-	-	4.08	0.08
9	2.21	0.02	2.73	0.03	2.81	0.04	-	-	3.97	0.05
10	2.71	0.02	2.94	0.05	3.41	0.07	-	-	4.29	0.11
11	2.18	0.05	2.51	0.04	2.85	0.04	-	-	3.70	0.08
12	1.96	0.03	2.56	0.04	2.35	0.05	-	-	3.61	0.03
13	2.37	0.03	2.78	0.03	3.21	0.08	-	-	4.01	0.05
14	2.11	0.01	2.52	0.04	2.86	0.06	-	-	3.50	0.04
16	2.54	0.02	2.94	0.06	3.35	0.07	-	-	4.21	0.09
17	2.63	0.03	3.07	0.03	3.48	0.05	-	-	4.39	0.03
18	2.76	0.04	3.16	0.04	3.61	0.04	-	-	4.46	0.09
19	2.82	0.02	3.32	0.03	3.80	0.05	-	-	4.61	0.09
20	2.05	0.02	3.14	0.05	2.85	0.03	-	-	4.65	0.12
21	2.34	0.03	2.76	0.02	3.07	0.06	-	-	3.93	0.06

22	2.67	0.02	3.16	0.07	3.60	0.08	-	-	4.48	0.03
23	2.41	0.05	2.80	0.07	3.29	0.03	-	-	4.07	0.09
24	2.95	0.05	3.40	0.04	3.95	0.03	-	-	4.83	0.11
26	2.38	0.02	2.77	0.02	3.16	0.06	-	-	3.86	0.03
28	2.90	0.07	3.34	0.03	3.82	0.05	-	-	4.77	0.06
29	3.02	0.04	3.60	0.09	4.21	0.03	-	-	5.07	0.10
30	3.03	0.05	3.69	0.03	4.20	0.08	-	-	5.21	0.03
31	3.05	0.05	3.66	0.06	4.23	0.04	-	-	5.20	0.04
32	3.18	0.03	3.68	0.03	4.28	0.04	-	-	5.34	0.06
33	3.21	0.03	3.73	0.05	4.21	0.03	-	-	5.10	0.11
34	3.19	0.02	3.68	0.04	4.31	0.03	-	-	5.21	0.09
36	2.86	0.04	3.44	0.07	3.87	0.03	-	-	4.78	0.07
37	2.87	0.05	3.36	0.07	3.83	0.08	-	-	4.66	0.10
38	2.62	0.06	3.42	0.03	3.33	0.09	-	-	4.87	0.04
39	2.95	0.04	3.38	0.08	4.02	0.09	-	-	4.69	0.05
40	2.22	0.04	2.82	0.06	3.40	0.07	-	-	4.12	0.10
41	1.62	0.03	2.00	0.02	1.32	0.05	-	-	2.71	0.07
42	2.64	0.04	3.18	0.04	3.65	0.03	-	-	4.44	0.03
43	2.84	0.03	3.38	0.04	3.94	0.06	-	-	4.76	0.04
44	2.71	0.02	3.19	0.03	3.65	0.05	-	-	4.39	0.09
45	2.70	0.05	3.20	0.02	3.64	0.03	-	-	4.53	0.07
46	2.78	0.03	3.25	0.08	3.64	0.09	-	-	4.64	0.03
47	2.42	0.04	3.09	0.03	3.07	0.08	-	-	4.29	0.04
48	2.73	0.06	3.22	0.07	3.73	0.05	-	-	4.12	0.05
49	2.27	0.02	2.70	0.02	3.08	0.07	-	-	3.87	0.07
50	3.10	0.05	3.20	0.06	4.11	0.10	-	-	5.01	0.05
51	2.59	0.03	2.96	0.07	3.45	0.05	-	-	4.22	0.10
52	3.27	0.06	3.84	0.03	4.42	0.04	-	-	5.47	0.04

53	3.11	0.03	3.65	0.03	4.11	0.10	-	-	5.14	0.10
54	3.21	0.03	3.77	0.09	4.37	0.07	-	-	5.26	0.06
55	2.83	0.05	3.34	0.04	3.84	0.07	-	-	4.82	0.08
56	2.65	0.02	3.40	0.07	3.67	0.02	-	-	4.57	0.07

Supporting Table 3. Characteristics of the overall rotational diffusion tensor of GB3 derived from ^{15}N relaxation data at different magnetic fields. Atom coordinates for this analysis were taken from the solution structures of GB3 refined using residual dipolar couplings (PDB entries 1P7E and 1P7F (Ulmer, T. S.; Ramirez, B. E.; Delaglio, F.; Bax, A. *J Am Chem Soc* **2003**, *125*, 9179-9191)). Numbers in the parentheses represent standard deviations.

Resonance frequency	D_{\perp}^{a}	D_{\parallel}^{a}	Φ^{b}	Θ^{b}	τ_c^{c}	Anisotropy ^d	$\chi^2/\text{df}^{\text{e}}$
<u>1P7E.pdb:</u>							
400 MHz	4.49(0.38)	6.15(1.42)	106(21)	63(22)	3.31(0.43)	1.37(0.31)	0.94
500 MHz	4.38(0.51)	6.25(1.92)	91(25)	63(32)	3.33(0.55)	1.43(0.41)	0.91
600 MHz	4.46(0.15)	6.03(0.43)	98(9)	60(13)	3.34(0.14)	1.35(0.09)	0.76
700 MHz	4.45(0.12)	6.23(0.38)	104(7)	54(13)	3.30(0.12)	1.40(0.08)	1.53
800 MHz	4.54(0.17)	6.02(0.48)	103(13)	53(21)	3.31(0.15)	1.33(0.09)	1.12
<u>1P7F.pdb:</u>							
400 MHz	4.48(0.38)	6.15(1.40)	103(20)	70(22)	3.31(0.42)	1.37(0.30)	0.94
500 MHz	4.38(0.51)	6.26(1.96)	90(23)	70(31)	3.33(0.56)	1.43(0.42)	0.90
600 MHz	4.46(0.15)	6.04(0.44)	96(9)	66(13)	3.34(0.14)	1.36(0.09)	0.73
700 MHz	4.44(0.13)	6.24(0.37)	100(7)	60(14)	3.31(0.12)	1.41(0.07)	1.58
800 MHz	4.54(0.17)	6.02(0.49)	100(13)	59(20)	3.31(0.15)	1.33(0.10)	1.12

^a Principal values (in 10^7 s^{-1}) of the rotational diffusion tensor.

^b Polar and azimuthal angles { Θ, Φ } (in degrees) describe the orientation of the diffusion tensor axis with respect to protein coordinate frame.

^c Overall rotational correlation time (in ns) of the molecule, $\tau_c = 1/[2 \text{ tr}(\underline{D})]$.

^d The degree of anisotropy of the diffusion tensor, D_{\parallel}/D_{\perp} .

^e Residuals of the fit divided by the number of degrees of freedom.

Supporting Table 4. Fully anisotropic overall rotational diffusion tensor of GB3 derived from ^{15}N relaxation data at different magnetic fields. Atom coordinates for this analysis were taken from the crystal structure of GB3 (PDB entry 1IGD) Numbers in the parentheses represent standard deviations.

Magnetic field (Tesla)	D_{xx}^{a} (10^7 s^{-1})	D_{yy}^{a} (10^7 s^{-1})	D_{zz}^{a} (10^7 s^{-1})	$\Phi^{\text{o b}}$	$\Theta^{\text{o b}}$	$\Psi^{\text{o b}}$	τ_c^{c} (ns)	Anisotropy ^d	Rhombicity ^e	$\chi^2/\text{df}^{\text{f}}$	P ^g
From auto- and cross-relaxation rate measurements											
9.4	4.17 (0.34)	4.56 (0.26)	6.32 (0.58)	87(16)	60 (12)	155(42)	3.33 (0.16)	1.45 (0.15)	0.30(0.06)	0.61	0.23
11.7	4.28 (0.16)	4.68 (0.28)	6.22 (0.49)	94(12)	77 (16)	141(28)	3.29 (0.13)	1.39 (0.12)	0.34(0.06)	0.58	0.04
14.1	4.39 (0.18)	4.54 (0.32)	6.03 (0.67)	91(13)	76 (19)	125(52)	3.34 (0.17)	1.35 (0.16)	0.14(0.03)	0.74	0.53
16.4	4.35 (0.19)	4.55 (0.24)	6.17 (0.40)	101(12)	62 (9)	95(51)	3.32 (0.11)	1.39 (0.10)	0.18(0.03)	0.88	0.43
18.8	4.44 (0.82)	4.49 (0.67)	6.15 (2.21)	101(20)	66 (10)	117 (259)	3.31 (0.54)	1.38 (0.52)	0.04(0.03)	0.79	0.92
	4.41	4.50	6.11	97	67	104	3.33	1.37	0.08	0.71	0.20
From cross-correlation rate measurements											
9.4	4.28 (0.33)	4.66 (0.24)	5.99 (0.40)	97(20)	67 (18)	130(63)	3.35 (0.13)	1.34 (0.11)	0.37(0.08)	0.61	0.15
11.7	4.24 (0.41)	4.48 (0.32)	6.22 (0.85)	90(14)	55 (11)	141(77)	3.34 (0.22)	1.43 (0.21)	0.19(0.05)	0.94	0.29
14.1	4.35 (0.25)	4.44 (0.20)	6.24 (0.66)	93(9)	65 (6)	169(53)	3.33 (0.16)	1.42 (0.16)	0.07(0.02)	0.54	0.83

Numbers in the parentheses represent standard deviations.

^a Principal values of the rotational diffusion tensor.

^b Euler angles $\{\Theta, \Phi, \Psi\}$ (in degrees) describe the orientation of the diffusion tensor axis with respect to protein coordinate frame.

^c Overall rotational correlation time of the molecule, $\tau_c = 1/[2 \text{ tr}(\underline{D})]$.

^d The degree of anisotropy of the diffusion tensor, $2D_{zz}/(D_{xx} + D_{yy})$.

^e The rhombicity of the diffusion tensor, $1.5(D_{yy} - D_{xx})/[D_{zz} - \frac{1}{2}(D_{xx} + D_{yy})]$

^f Residuals of the fit divided by the number of degrees of freedom.

^g Probability that the reduction in χ^2 (compared to the axially symmetric model) occurred by chance. For comparison, similar probabilities for the fully anisotropic versus isotropic diffusion tensor model range from $P=7 \times 10^{-10}$ (at 9.4 T) to $P=6 \times 10^{-17}$ (at 16.4 T). The numbers for the axially symmetric versus isotropic model are presented in Table 2 (text).

Supporting Table 5a. Site-specific components of the ^{15}N chemical shift tensor (assumed axially symmetric) in GB3. Here: $\delta_{\parallel} = \delta_{\text{iso}} + 2\Delta\delta / 3$ and $\delta_{\perp} = \delta_{\text{iso}} - \Delta\delta / 3$, were calculated from the experimentally determined $\Delta\delta_{\text{iso}}$ and $\Delta\sigma$ (average over three methods) using the relationships $\Delta\delta = \delta_{\parallel} - \delta_{\perp}$, $\delta_{\text{iso}} = (2\delta_{\perp} + \delta_{\parallel}) / 3$, and $\Delta\sigma = -\Delta\delta$. Numbers in the parentheses represent experimental uncertainties in the corresponding parameters; the experimental errors in δ_{iso} are assumed to be negligible relative to the errors in $\Delta\delta$.

Residue	$\Delta\delta$	δ_{iso}	δ_{\parallel}	δ_{\perp}
2	195.94 (5.23)	123.13	253.76 (3.48)	57.81 (1.74)
3	168.11 (6.85)	123.87	235.95 (4.57)	67.84 (2.28)
4	159.82 (8.08)	122.34	228.88 (5.38)	69.06 (2.69)
5	168.7 (7.78)	126.29	238.76 (5.19)	70.06 (2.59)
6	162.06 (7.56)	126.87	234.91 (5.04)	72.85 (2.52)
7	160.36 (9.71)	125.32	232.22 (6.47)	71.87 (3.24)
8	177.36 (9.19)	128.83	247.07 (6.12)	69.71 (3.06)
9	172.46 (4.49)	110.05	225.03 (2.99)	52.57 (1.50)
10	193.68 (7.18)	120.44	249.56 (4.79)	55.88 (2.39)
11	186.81 (7.72)	108.68	233.22 (5.15)	46.41 (2.57)
12	111.26 (1.71)	125.43	199.61 (1.14)	88.35 (0.57)
13	158.6 (5.78)	123.36	229.09 (3.85)	70.49 (1.93)
14	191.5 (9.05)	109.06	236.72 (6.03)	45.22 (3.02)
16	166.83 (12.36)	115.45	226.67 (8.24)	59.84 (4.12)
17	187.32 (8.52)	111.54	236.41 (5.68)	49.1 (2.84)
18	178.31 (7.02)	114.84	233.71 (4.68)	55.4 (2.34)

19	172.59 (7.72)	124.03	239.08 (5.14)	66.5 (2.57)
20	128.09 (2.04)	124.38	209.77 (1.36)	81.68 (0.68)
21	186.34 (5.33)	115.24	239.47 (3.55)	53.13 (1.78)
22	179.31 (8.97)	115.11	234.65 (5.98)	55.34 (2.99)
23	168.95 (8.03)	120.88	233.51 (5.35)	64.56 (2.68)
24	191.21 (8.63)	118.73	246.2 (5.76)	54.99 (2.88)
26	136.01 (13.94)	125.00	215.67 (9.29)	79.66 (4.65)
28	174.16 (11.56)	116.20	232.31 (7.71)	58.15 (3.85)
29	160.03 (11.41)	121.97	228.65 (7.61)	68.62 (3.80)
30	192.95 (7.96)	119.51	248.14 (5.31)	55.2 (2.65)
31	184.55 (8.3)	122.67	245.7 (5.54)	61.15 (2.77)
32	185.17 (8.19)	119.39	242.83 (5.46)	57.66 (2.73)
33	196.28 (9.74)	120.19	251.04 (6.49)	54.76 (3.25)
34	185.03 (7.94)	122.28	245.63 (5.29)	60.6 (2.65)
36	161.59 (5.71)	121.00	228.73 (3.81)	67.14 (1.9)
37	173.19 (7.51)	115.09	230.56 (5.01)	57.36 (2.5)
38	138.95 (4.05)	107.95	200.59 (2.7)	61.63 (1.35)
40	163.32 (1.5)	127.72	236.61 (1.00)	73.28 (0.50)
41	154.88 (0.84)	107.04	210.29 (0.56)	55.41 (0.28)
42	176.23 (10.22)	120.20	237.68 (6.81)	61.46 (3.41)
43	203.35 (5.34)	130.83	266.4 (3.56)	63.05 (1.78)
44	180.2 (6.41)	114.42	234.55 (4.27)	54.36 (2.14)
45	179.82 (6.83)	119.97	239.85 (4.55)	60.03 (2.28)
46	190.59 (8.77)	128.11	255.17 (5.85)	64.58 (2.92)
47	154.85 (4.01)	124.68	227.91 (2.67)	73.07 (1.34)
48	215.48 (1.77)	119.61	263.26 (1.18)	47.78 (0.59)
49	131.07 (4.04)	102.95	190.33 (2.69)	59.26 (1.35)
50	187.75 (4.98)	122.77	247.93 (3.32)	60.18 (1.66)

51	175.59 (8.09)	111.02	228.08 (5.39)	52.49 (2.70)
52	240.76 (11.05)	130.91	291.41 (7.37)	50.66 (3.68)
53	192.8 (9.6)	117.40	245.93 (6.4)	53.13 (3.20)
54	181.43 (5.13)	122.99	243.95 (3.42)	62.51 (1.71)
55	164.08 (6.59)	123.88	233.26 (4.39)	69.18 (2.2)
56	162.96 (5.66)	133.42	242.07 (3.78)	79.1 (1.89)

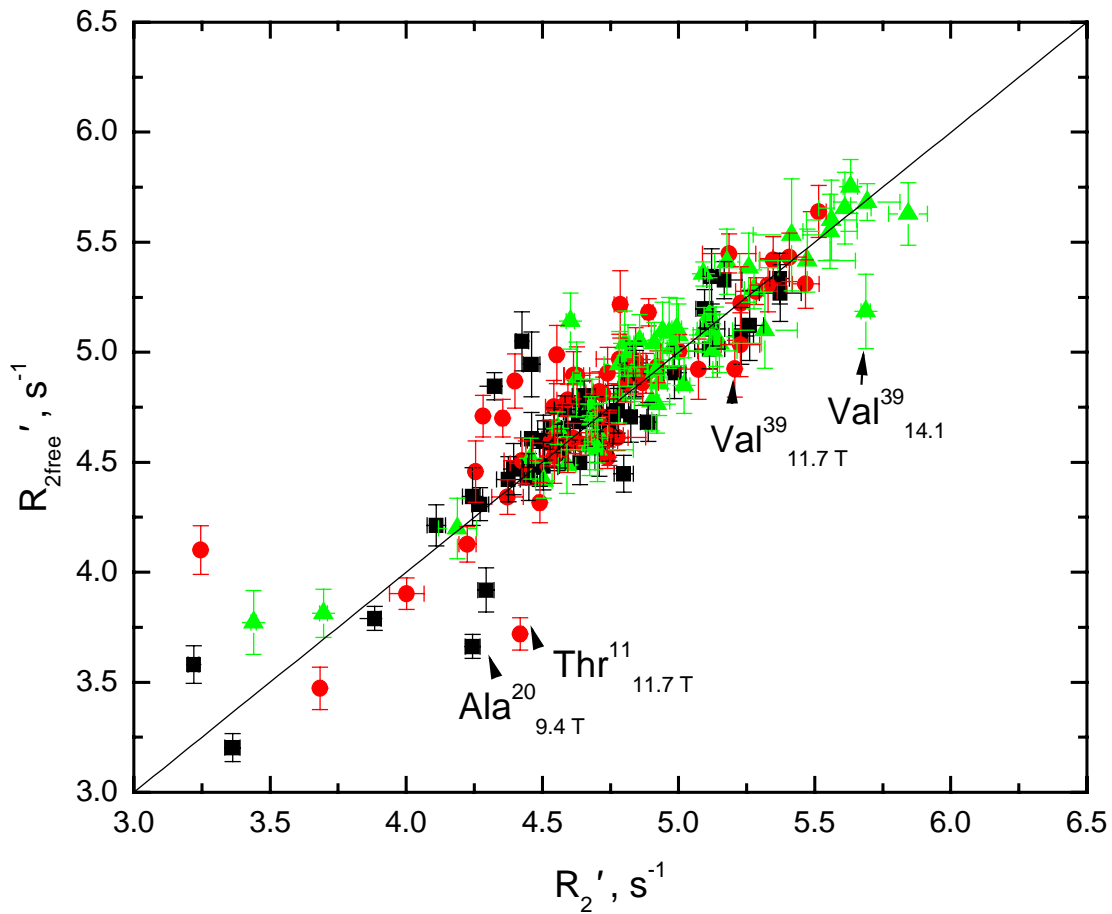
Supporting Table 5b. Site-specific components of the ^{15}N chemical shielding tensor

(assumed axially symmetric) in GB3. These values were calculated from the derived values of $\Delta\sigma$ assuming a traceless chemical shielding tensor (i.e. $2\sigma_{\perp} + \sigma_{\parallel} = 0$): $\sigma_{\parallel} = 2\Delta\sigma/3$ and $\sigma_{\perp} = -\Delta\sigma/3$. These values are related to the chemical shift tensor components presented in Supporting Table 5a via the following equations: $\delta_{\parallel} = \delta_{\text{iso}} - \sigma_{\parallel}$ and $\delta_{\perp} = \delta_{\text{iso}} - \sigma_{\perp}$. Numbers in the parentheses represent experimental uncertainties in the corresponding parameters.

Residue	$\Delta\sigma$	σ_{\parallel}	σ_{\perp}
2	-195.94 (5.23)	-130.63 (3.48)	65.31 (1.74)
3	-168.11 (6.85)	-112.07 (4.57)	56.04 (2.28)
4	-159.82 (8.08)	-106.55 (5.38)	53.27 (2.69)
5	-168.7 (7.78)	-112.46 (5.19)	56.23 (2.59)
6	-162.06 (7.56)	-108.04 (5.04)	54.02 (2.52)
7	-160.36 (9.71)	-106.91 (6.47)	53.45 (3.24)
8	-177.36 (9.19)	-118.24 (6.12)	59.12 (3.06)
9	-172.46 (4.49)	-114.97 (2.99)	57.49 (1.5)
10	-193.68 (7.18)	-129.12 (4.79)	64.56 (2.39)
11	-186.81 (7.72)	-124.54 (5.15)	62.27 (2.57)
12	-111.26 (1.71)	-74.17 (1.14)	37.09 (0.57)
13	-158.6 (5.78)	-105.73 (3.85)	52.87 (1.93)

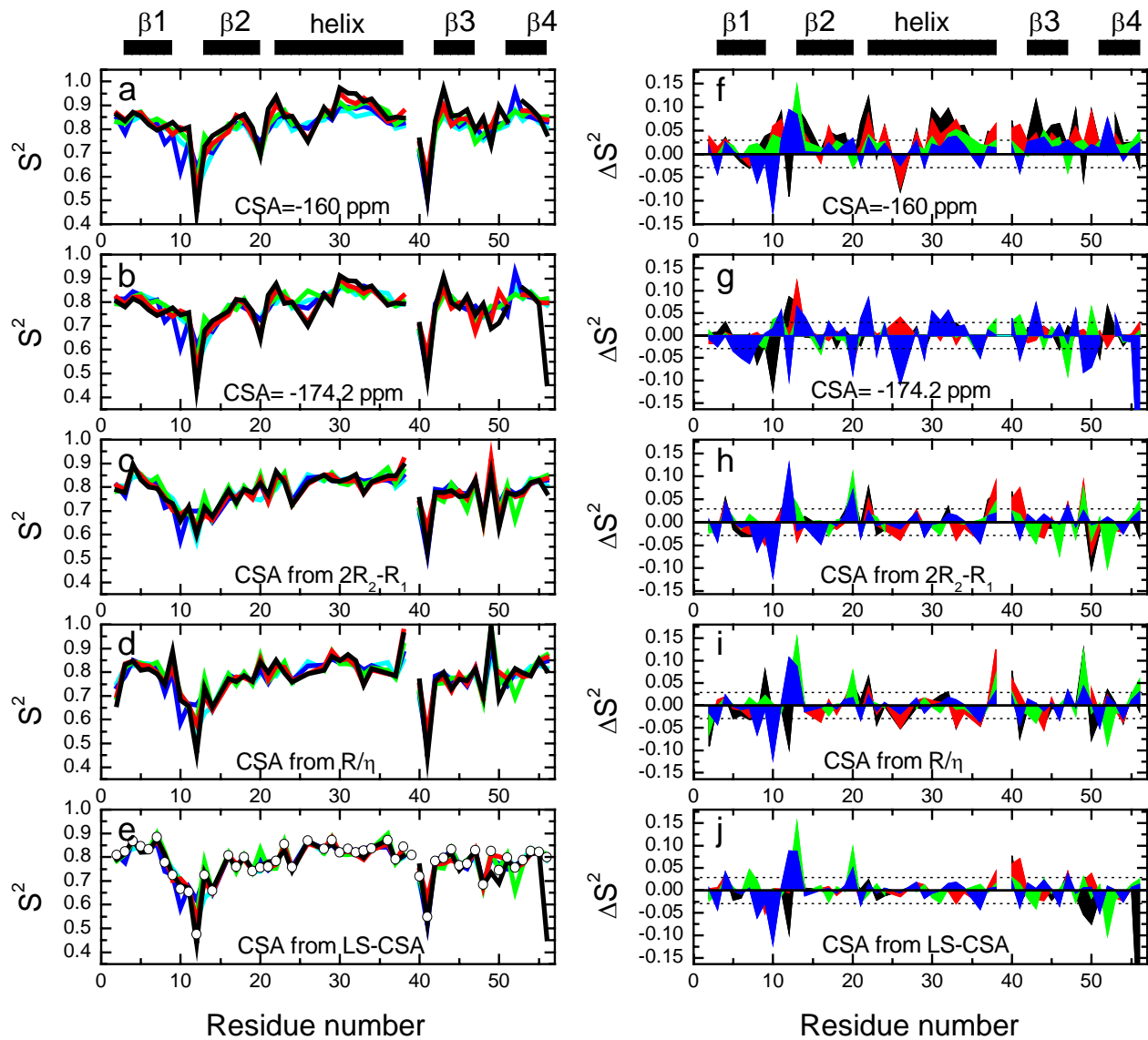
14	-191.5 (9.05)	-127.66 (6.03)	63.83 (3.02)
16	-166.83 (12.36)	-111.22 (8.24)	55.61 (4.12)
17	-187.32 (8.52)	-124.88 (5.68)	62.44 (2.84)
18	-178.31 (7.02)	-118.87 (4.68)	59.44 (2.34)
19	-172.59 (7.72)	-115.06 (5.14)	57.53 (2.57)
20	-128.09 (2.04)	-85.39 (1.36)	42.7 (0.68)
21	-186.34 (5.33)	-124.23 (3.55)	62.11 (1.78)
22	-179.31 (8.97)	-119.54 (5.98)	59.77 (2.99)
23	-168.95 (8.03)	-112.63 (5.35)	56.32 (2.68)
24	-191.21 (8.63)	-127.48 (5.76)	63.74 (2.88)
26	-136.01 (13.94)	-90.68 (9.29)	45.34 (4.65)
28	-174.16 (11.56)	-116.11 (7.71)	58.05 (3.85)
29	-160.03 (11.41)	-106.69 (7.61)	53.34 (3.8)
30	-192.95 (7.96)	-128.63 (5.31)	64.32 (2.65)
31	-184.55 (8.3)	-123.03 (5.54)	61.52 (2.77)
32	-185.17 (8.19)	-123.45 (5.46)	61.72 (2.73)
33	-196.28 (9.74)	-130.86 (6.49)	65.43 (3.25)
34	-185.03 (7.94)	-123.35 (5.29)	61.68 (2.65)
36	-161.59 (5.71)	-107.73 (3.81)	53.86 (1.9)
37	-173.19 (7.51)	-115.46 (5.01)	57.73 (2.5)
38	-138.95 (4.05)	-92.63 (2.70)	46.32 (1.35)
40	-163.32 (1.5)	-108.88 (1.00)	54.44 (0.5)
41	-154.88 (0.84)	-103.25 (0.56)	51.63 (0.28)
42	-176.23 (10.22)	-117.48 (6.81)	58.74 (3.41)
43	-203.35 (5.34)	-135.57 (3.56)	67.78 (1.78)
44	-180.2 (6.41)	-120.13 (4.27)	60.07 (2.14)
45	-179.82 (6.83)	-119.88 (4.55)	59.94 (2.28)
46	-190.59 (8.77)	-127.06 (5.85)	63.53 (2.92)

47	-154.85 (4.01)	-103.23 (2.67)	51.62 (1.34)
48	-215.48 (1.77)	-143.65 (1.18)	71.83 (0.59)
49	-131.07 (4.04)	-87.38 (2.69)	43.69 (1.35)
50	-187.75 (4.98)	-125.17 (3.32)	62.58 (1.66)
51	-175.59 (8.09)	-117.06 (5.39)	58.53 (2.7)
52	-240.76 (11.05)	-160.5 (7.37)	80.25 (3.68)
53	-192.8 (9.6)	-128.53 (6.4)	64.27 (3.2)
54	-181.43 (5.13)	-120.96 (3.42)	60.48 (1.71)
55	-164.08 (6.59)	-109.38 (4.39)	54.69 (2.2)
56	-162.96 (5.66)	-108.64 (3.78)	54.32 (1.89)



Supporting Figure 1. The agreement between measured R_2' and their reconstructed “exchange-free” values, $R_{2\text{free}'} = R_1' \cdot \eta_{xy}/\eta_z$.

Shown is the agreement between the values of R_2' and $R_{2\text{free}'}$ in GB3 at 9.4 T (black squares), 11.7 T (red circles) and 14.1 T (green triangles). Here R_{ex} contributions are expected to shift the data points to the right of the diagonal; with the magnitude of the shift proportional to the square of the strength of the static magnetic field. The only residues that show noticeable right shifts in GB3 are indicated with arrows and text labels. Ala20 shows a large shift to the right at 9.4 T, but no such shift at higher fields, which suggests that this shift is most likely due to experimental errors rather than real R_{ex} contribution. Similar considerations apply to the large shift of Thr11 at 11.7 T. Only Val39 in GB3 has a shift that gets increasingly larger with field strength.



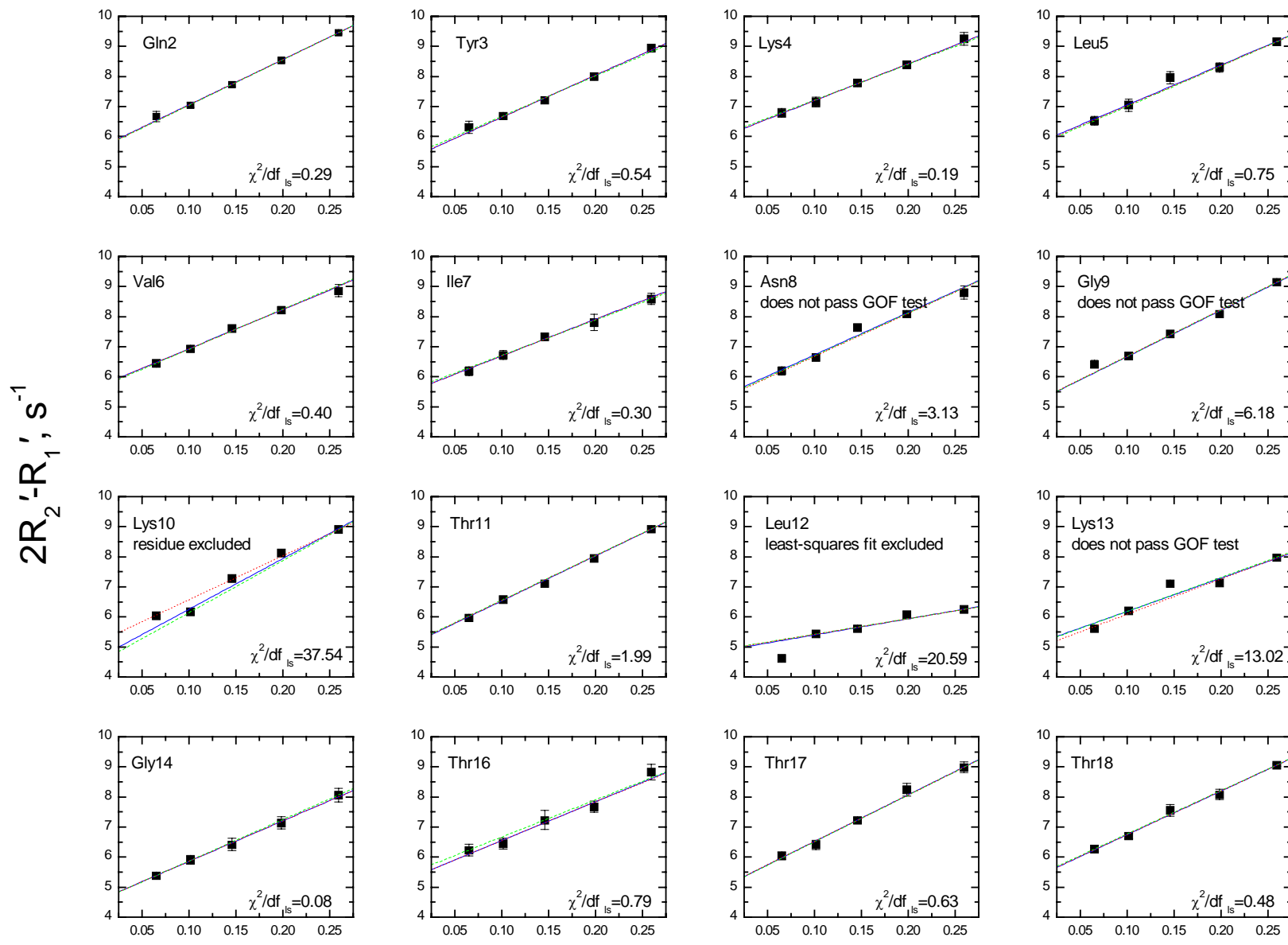
Supporting Figure 2. Backbone order parameters determined from model-free analysis of ^{15}N relaxation data at each field using different CSA models and allowing full freedom in the LS model selection.

The organization of the panels in this figure is similar to Figure 6 in the main text. The difference is that here model selection for a given amide group was performed for each field independently, and no restriction on the model selection was applied, except the natural one following from the available number of degrees of freedom.

Shown are backbone order parameters in GB3 derived from a LS analysis of the ^{15}N relaxation data (R_1 , R_2 , NOE) at different fields (left panels). Right panels represent the differences, $\Delta S^2 = S^2 - S^2(9.4\text{T})$, between the S^2 values at a particular field and at 9.4 Tesla, where the ^{15}N CSA contribution to ^{15}N relaxation rates is the weakest. **(a, f)** The LS analysis was performed in a conventional way, i.e. assuming a uniform CSA of -160 ppm for all residues. **(b, g)** The LS analysis was performed assuming a uniform CSA of -174.2 ppm (the average of the site-specific CSAs in GB3) for all residues. **(c, h)** Site-specific ^{15}N CSA values from the $2R_2-R_1$ method were used as input parameters. **(d, i)** Site-specific ^{15}N CSA values from the R/η method were used as input parameters. **(e, j)** The LS analysis was performed for each field separately using the site-specific CSAs derived from the global fit (LS-CSA) of all five fields. Also shown as open circles in panel (d) are the order parameters from the global fit. The coloring is as follows: the 18.8T data are shown in black, 16.4 T in red, 14.1 T in green, 11.7 T in blue, and 9.4 T data in cyan. The dashed horizontal lines represent the average estimated level (± 0.029) of the experimental uncertainty in ΔS^2 . Val39 has been removed from all panels because of the conformational exchange contribution.

Supporting Figure 3 (see next 4 pages). Fits of the dependence of $2R_2' - R_1'$ on ω_{N}^2 .

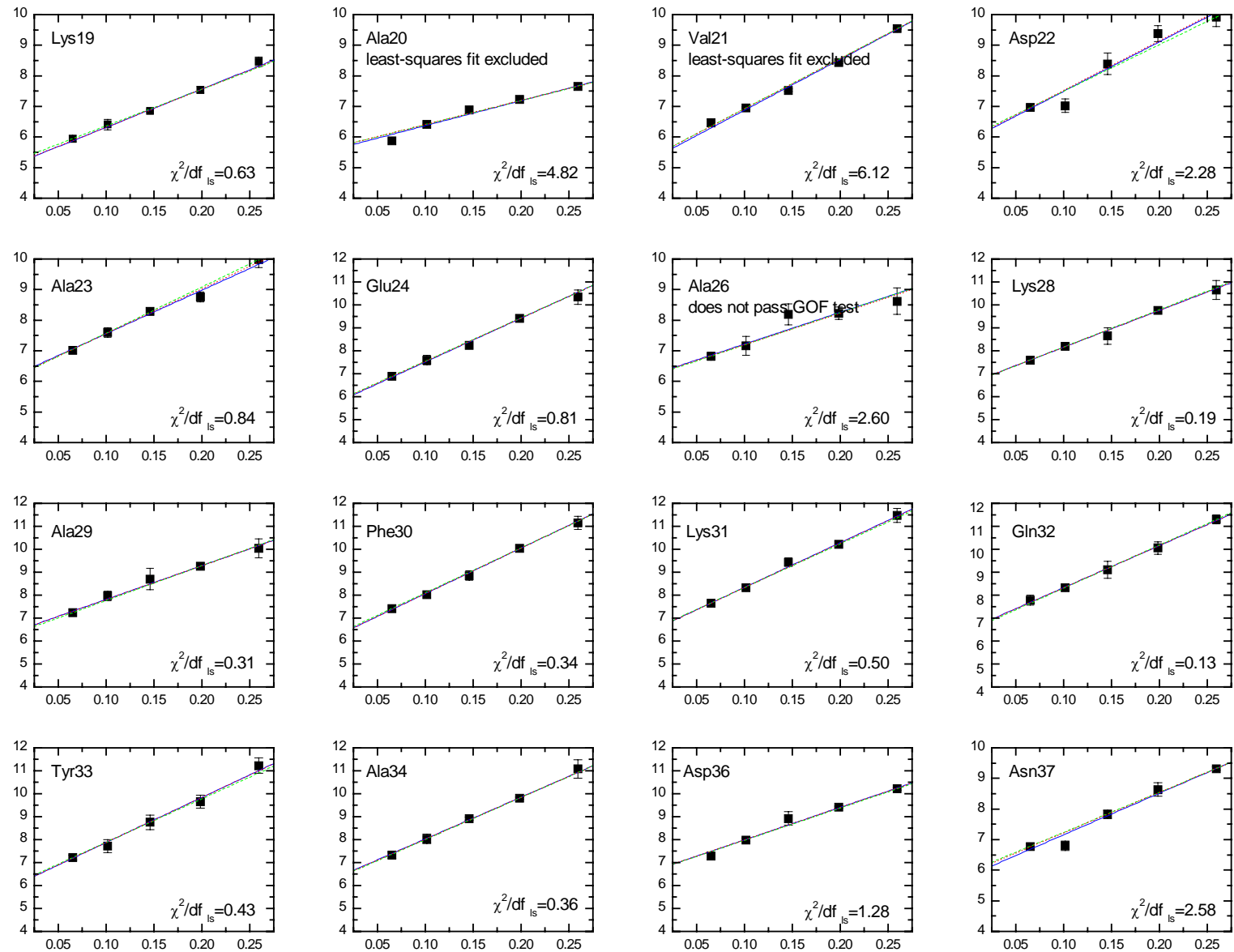
Shown are fits from the $2R_2-R_1$ method for all residues in GB3. The blue lines are the least-squares fit lines, the dashed green lines are the absolute value ($\rho(z) = |z|$, see text) robust method fit lines, the dotted red lines are the logarithm robust method fit lines ($\rho(z) = \log(1 + \frac{1}{2}z^2)$, see text). The value of χ^2/df for the least-squares fit is given in the lower right corner of each panel. The 95% confidence level χ^2/df cutoff for this fit (which has 3 degrees of freedom for a typical data set here) is 2.60.



Supp. Fig.3, continued

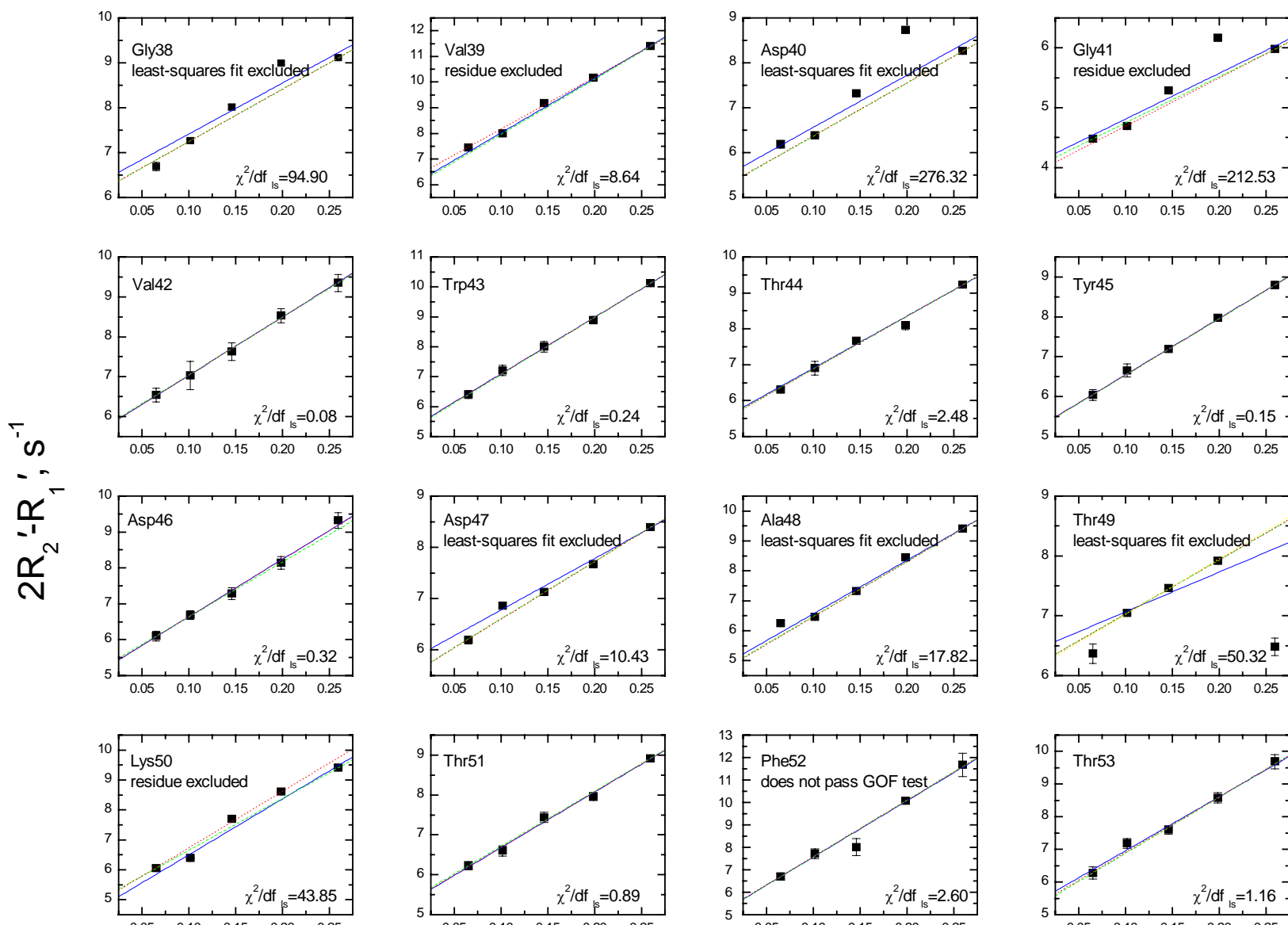
$$\omega_N^2, 10^{18}(\text{rad/s})^2$$

$2R_2' - R_1', \text{ s}^{-1}$



Supp. Fig.3, continued

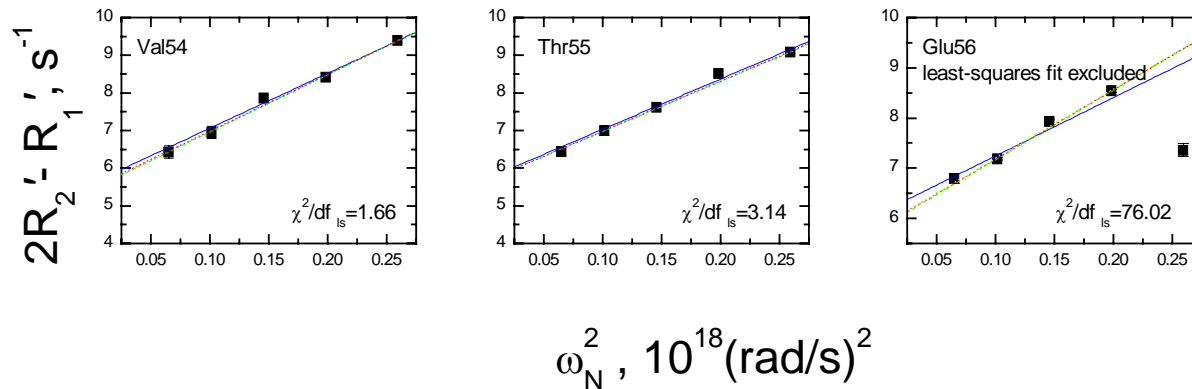
$$\omega_N^2, 10^{18}(\text{rad/s})^2$$



Supp. Fig.3, continued

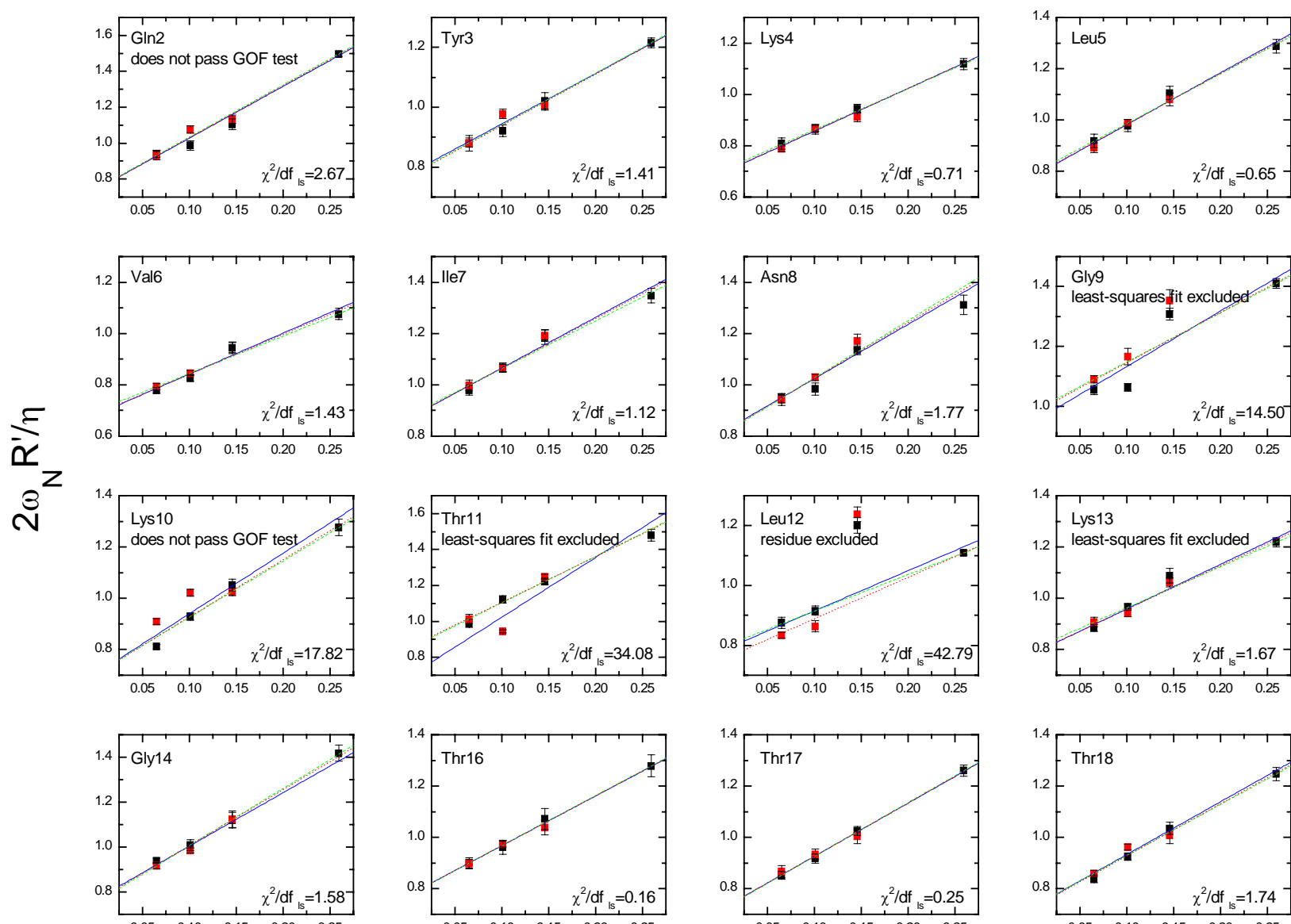
$$\omega_N^2, 10^{18}(\text{rad/s})^2$$

Supp. Fig.3, continued



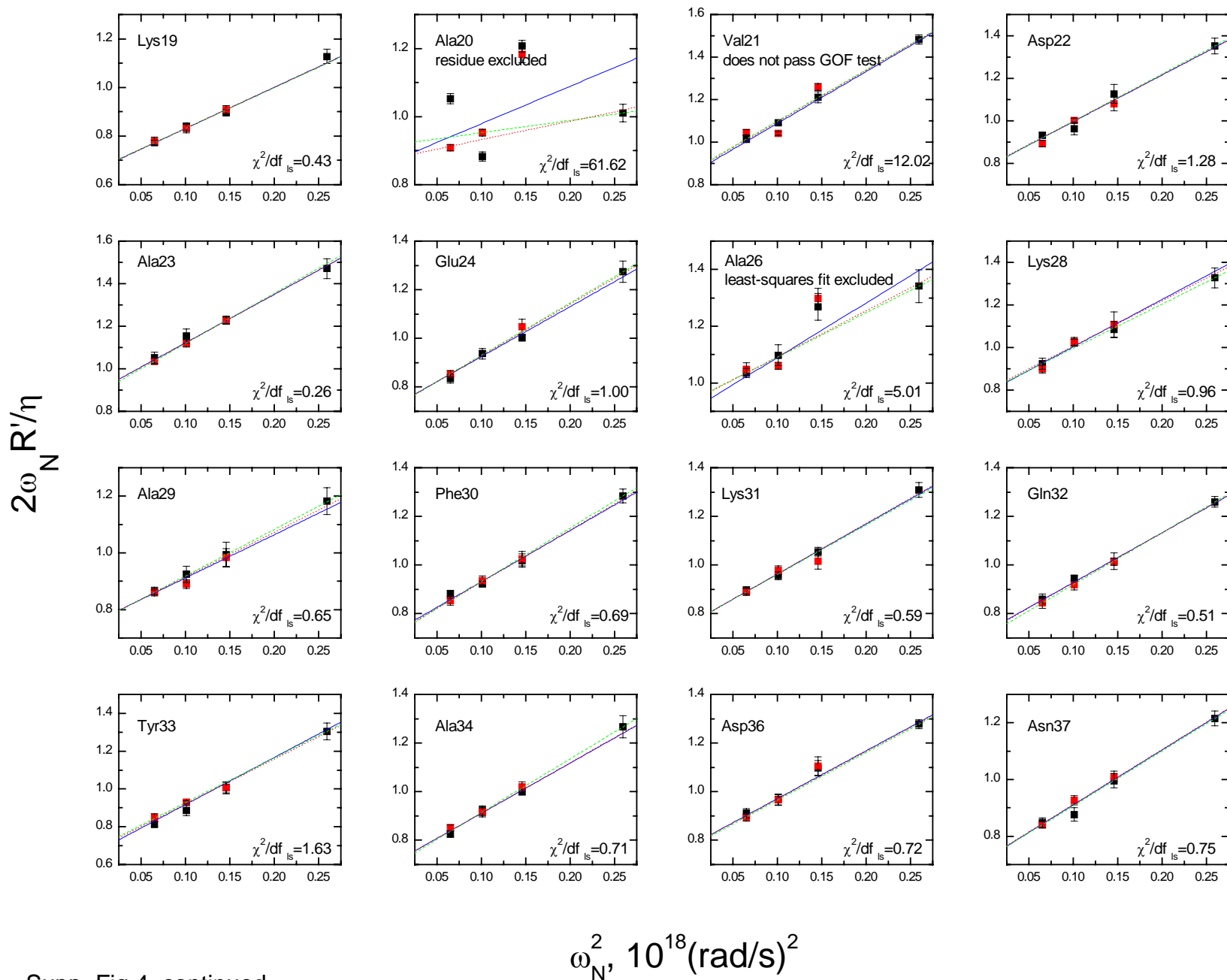
Supporting Figure 4 (next 4 pages). Fits of the dependence of $2\omega_N R'/\eta$ on ω_N^2 .

Shown are fits from the R/η method for all residues in GB3. As in Supporting Fig. 3, blue lines are the least-squares fit lines, dashed green lines are the absolute value robust method fit lines, dotted red lines are the logarithm robust method fit lines. The χ^2/df value for the least-squares fit is given in the lower right corner of each panel. The 95% confidence χ^2/df cutoff for this fit (which has 5 degrees of freedom for a typical data set here) is 2.21.



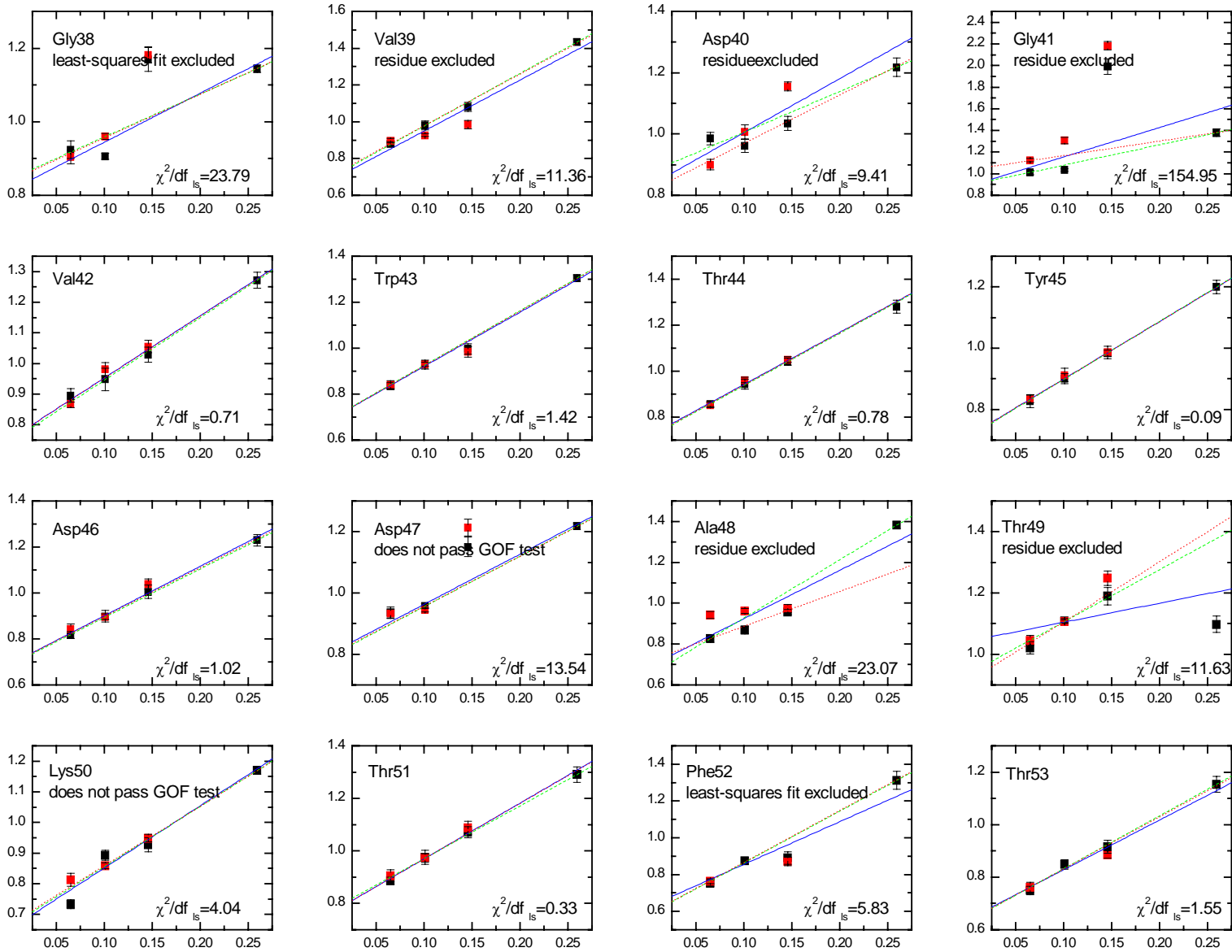
Supp. Fig.4, continued

$$\omega_N^2, 10^{18}(\text{rad/s})^2$$



Supp. Fig.4, continued

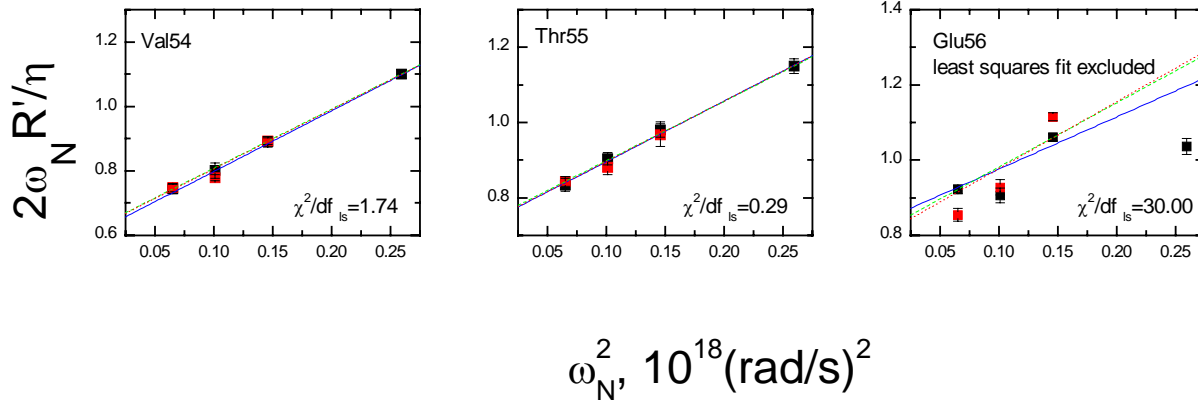
$2\omega_N R' / \eta$



$\omega_N^2, 10^{18}(\text{rad/s})^2$

Supp. Fig.4, continued

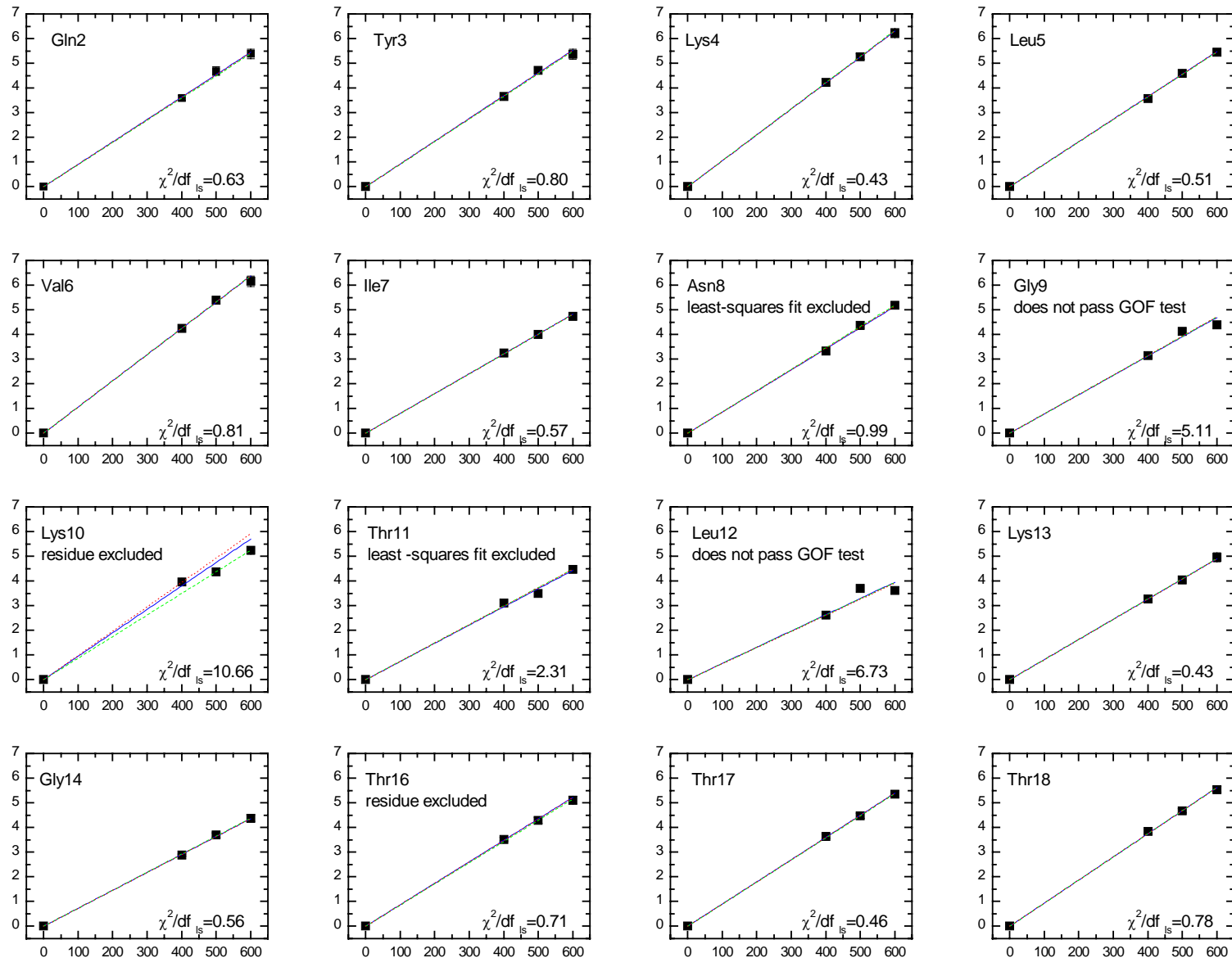
Supp. Fig.4, continued



Supporting Figure 5 (next 4 pages). Fits of the dependence of $2\eta_{xy} - \eta_z$ on the spectrometer frequency (in MHz).

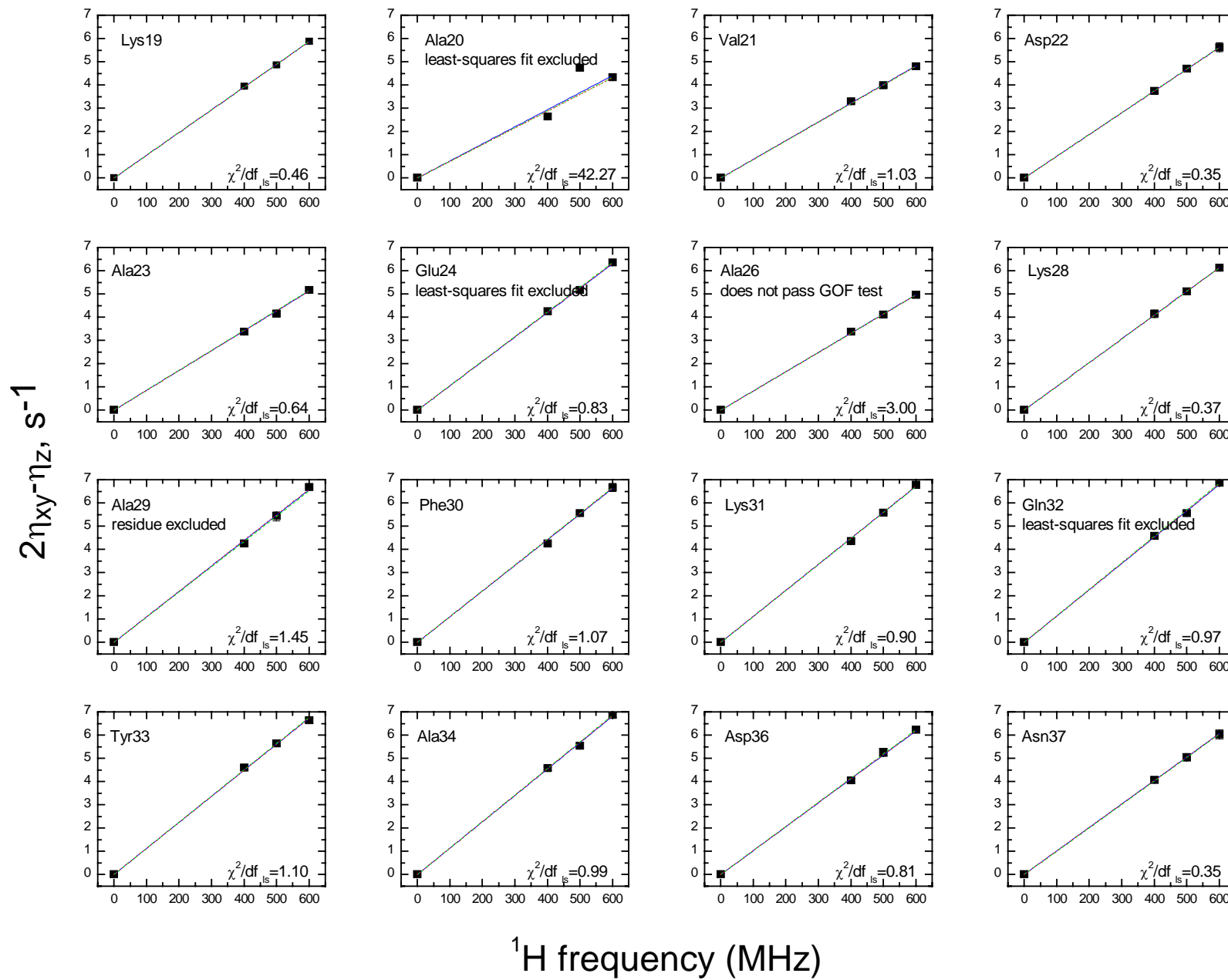
Shown are fits from the $2\eta_{xy} - \eta_z$ method for all residues in GB3. Blue lines are the least-squares fit lines, dashed green lines are the absolute value robust method fit lines, dotted red lines are the logarithm robust method fit lines. The χ^2/df for the least-squares fit is given in the lower right corner of each panel. The 95% confidence χ^2/df cutoff for this fit (which has 2 degrees of freedom for a typical data set here) is 3.00.

$2\eta_{xy}\eta_z \text{ s}^{-1}$



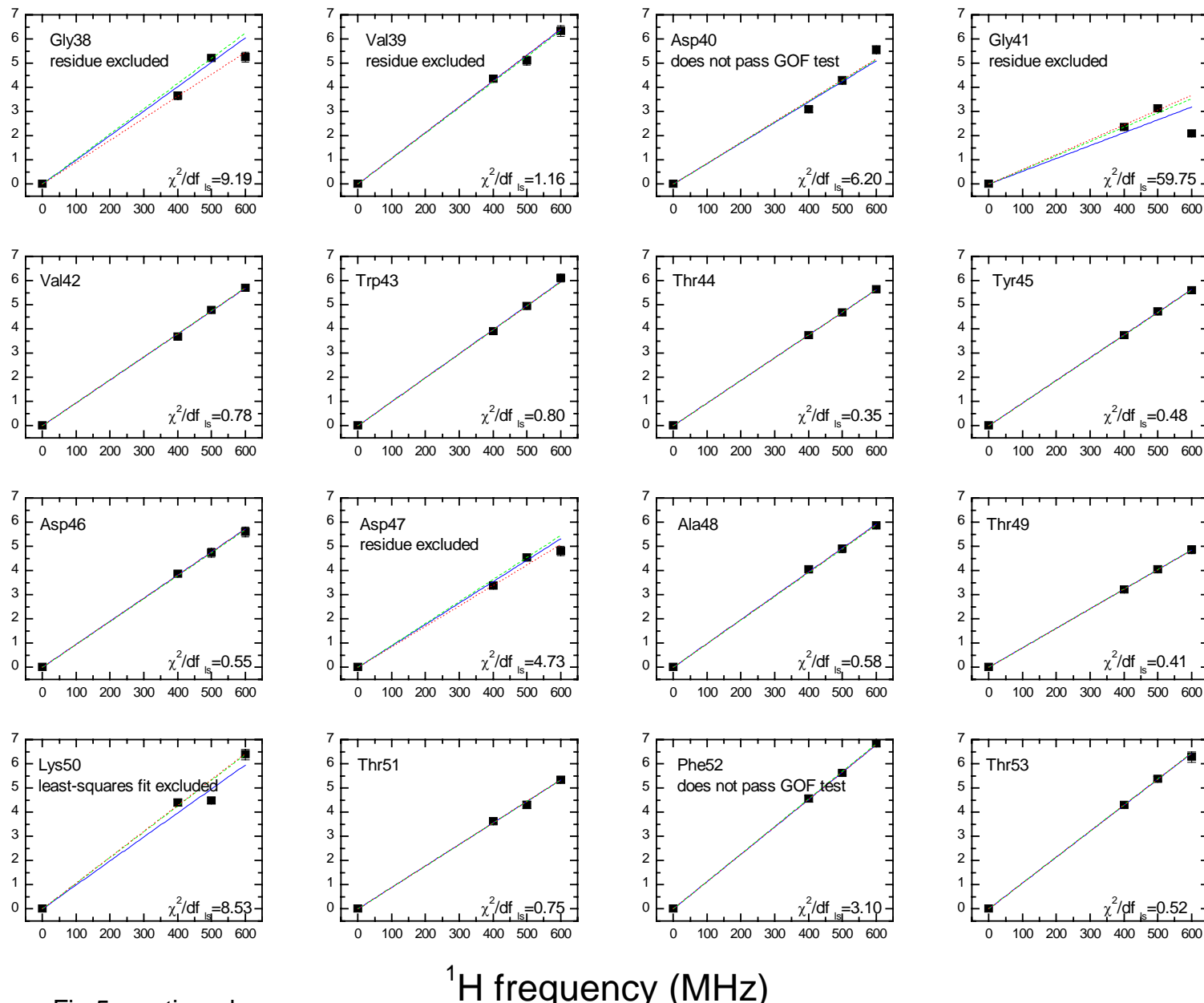
Supp. Fig.5, continued

^1H frequency (MHz)



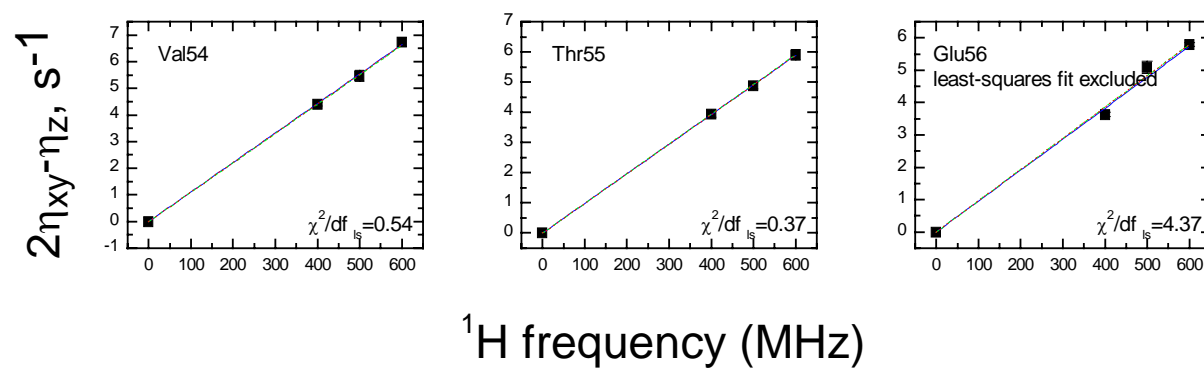
Supp. Fig.5, continued

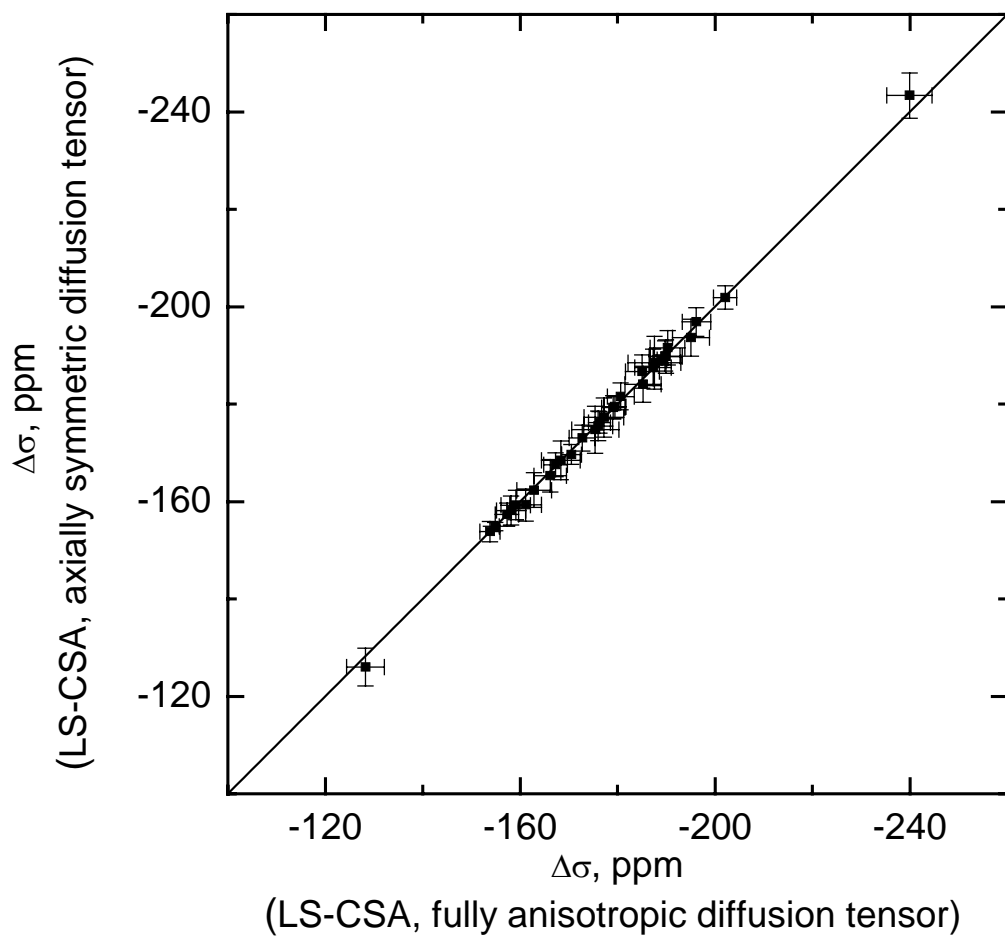
$2\eta_{xy}\cdot\eta_z$, s⁻¹



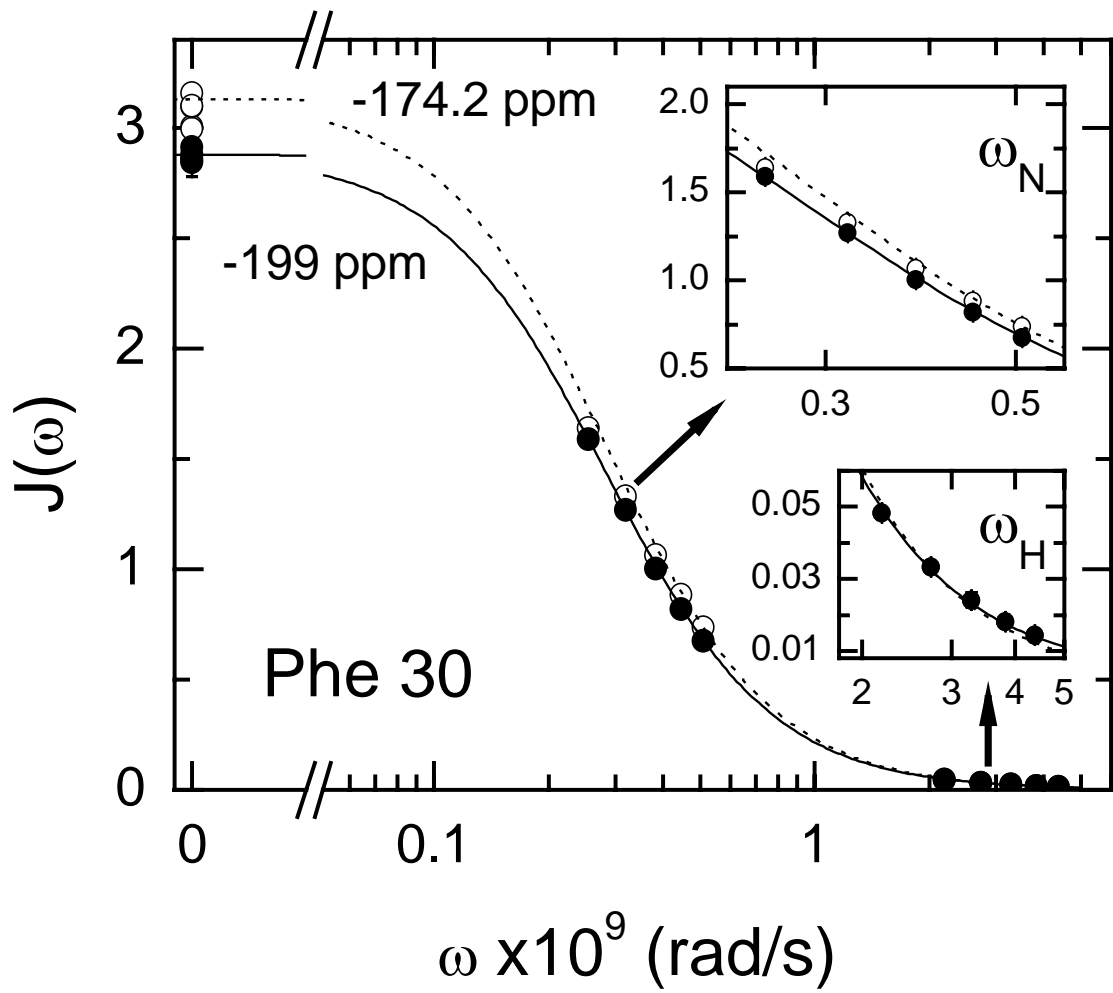
Supp. Fig.5, continued

Supp. Fig.5, continued



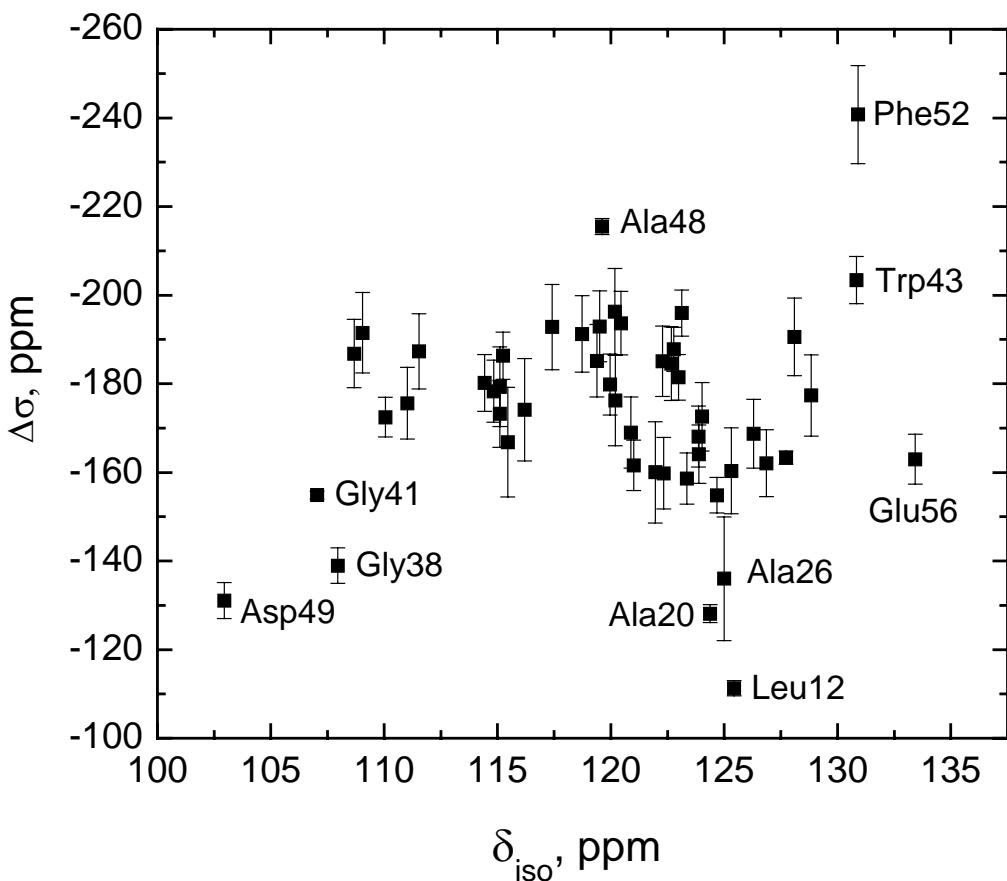


Supporting Figure 6. Comparison of CSAs from LS-CSA method, using fully anisotropic and axially symmetric overall rotational diffusion tensor. Shown are data for GB3 residues belonging to the secondary structure.



Supporting Figure 7. Illustration of the LS fit of the spectral density components determined at all five fields.

Representative LS fit of all spectral density components from the five-field measurements for Phe30 using site-specific CSA compared with fit using CSA = -174.2 . The values of S^2 and τ_{loc} were 0.89 and 7.4 ps when using CSA of -174.2 ppm. The χ^2/df for this fit is 6.10. This corresponds to a 12-fold greater χ^2/df compared to the fit using the CSA value of -199.1 ppm which optimizes the fit.



Supporting Figure 8. Comparison of ^{15}N CSAs with isotropic chemical shifts in GB3.

There is no obvious correlation with the isotropic chemical shifts although some residues with large $|\Delta\sigma|$, in particular Phe52 and Trp43, do show large isotropic shifts, while Asp49 and Gly38 have both small isotropic chemical shifts and $|\Delta\sigma|$.